

1 **Climatological variations of total alkalinity and total dissolved inorganic carbon in the**
2 **Mediterranean Sea surface waters**

3
4 **GEMAYEL Elissar^{1,2,3}, HASSOUN Abed El Rahman³, BENALLAL Mohamed Anis^{1,2},**
5 **GOYET Catherine^{1,2}, RIVARO Paola⁴, ABOUD-ABI SAAB Marie³,**
6 **KRASAKOPOULOU Evangelina⁵, TOURATIER Franck^{1,2} and ZIVERI Patrizia^{6,7}**

7
8 ¹ Université de Perpignan Via Domitia, IMAGES_ESPACE-DEV, 52 avenue Paul Alduy, 66860 Perpignan Cedex 9, France

9 ² ESPACE-DEV, UG UA UR UM IRD, Maison de la télédétection, 500 rue Jean-François Breton, 34093 Montpellier Cedex
10 5, France

11 ³ National Council for Scientific Research, National Center for Marines Sciences, P.O Box 534, Batroun, Lebanon

12 ⁴ University of Genova, Department of Chemistry and Industrial Chemistry, via Dodecaneso 31, 16146 Genova, Italy

13 ⁵ University of the Aegean, Department of Marine Sciences, University Hill, Mytilene 81100, Greece

14 ⁶ Universitat Autònoma de Barcelona, Institute of Environmental Science and Technology, Barcelona, Spain

15 ⁷ Universiteit Amsterdam, Earth & Climate Cluster, Department of Earth Sciences, Faculty of Earth and Life Sciences,
16 Amsterdam, The Netherlands

17
18 Correspondence: Elissar GEMAYEL

19 Permanent address: National Council for Scientific Research, National Center for Marines Sciences, P.O Box 534, Batroun,
20 Lebanon

21 Mobile: +961 70794882

22 Email: elissargemayel@hotmail.com

23
24 **Abstract**

25
26 A compilation of several cruises data from 1998 to 2013 was used to derive polynomial fits
27 that estimate total alkalinity (A_T) and total dissolved inorganic carbon (C_T) from
28 measurements of salinity and temperature in the Mediterranean Sea surface waters. The
29 optimal equations were chosen based on the 10-fold cross validation results and revealed that
30 a second and third order polynomials fit the A_T and C_T data respectively. The A_T surface fit
31 yielded a root mean square error (RMSE) of $\pm 10.6 \mu\text{mol.kg}^{-1}$, and salinity and temperature
32 contribute to 96% of the variability. Furthermore we present the first annual mean C_T
33 parameterization for the Mediterranean Sea surface waters with a RMSE of $\pm 14.3 \mu\text{mol.kg}^{-1}$.
34 Excluding the marginal seas of the Adriatic and the Aegean, these equations can be used to
35 estimate A_T and C_T in case of the lack of measurements. The identified empirical equations
36 were applied on the quarter degree climatologies of temperature and salinity, available from
37 the World Ocean Atlas 2013. The seven years averages (2005-2012) showed that A_T and C_T
38 have similar patterns with an increasing Eastward gradient. The variability is influenced by
39 the inflow of cold Atlantic waters through the Strait of Gibraltar and by the oligotrophic and
40 thermohaline gradient that characterize the Mediterranean Sea. The summer-winter
41 seasonality was also mapped and showed different patterns for A_T and C_T . During the winter,
42 the A_T and C_T concentrations were higher in the Western than in the Eastern basin. The
43 opposite was observed in the summer where the Eastern basin was marked by higher A_T and
44 C_T concentrations than in winter. The strong evaporation that takes place in this season along
45 with the ultra-oligotrophy of the Eastern basin determines the increase of both A_T and C_T
46 concentrations.

48 **Keywords:** Mediterranean Sea; Carbonate System; Surface Waters; Empirical Modeling;
49 Seasonal Variations

50

51 **1. Introduction**

52

53 The role of the ocean in mitigating climate change is well known as it absorbs about 2 Pg C
54 yr⁻¹ of anthropogenic CO₂ (Wanninkhof et al., 2013). Worldwide measurements of surface
55 seawater CO₂ properties are being conducted as they are important for advancing our
56 understanding of the carbon cycle and the underlying processes controlling it. For instance,
57 the buffer capacity of the CO₂ system varies with temperature, the distribution of total
58 inorganic carbon and total alkalinity (Omta et al., 2011).

59

60 Our understanding of the open-ocean CO₂ dynamics has drastically improved over the years
61 (Rödenbeck et al., 2013; Sabine et al., 2004; Takahashi et al., 2009; Watson and Orr, 2003).
62 However our understanding of marginal seas such as the Mediterranean remains poor due to
63 the limited measurements combined with the enhanced complexity of the land-ocean
64 interactions. In the Mediterranean Sea, available measurements of the carbonate system are
65 still scarce and only available in specific regions such as the Alboran sea (Copin-Montégut,
66 1993), the Gibraltar Strait (Santana-Casiano et al., 2002), the Dyfamed time-series in the
67 Ligurian Sea (Bégovic and Copin-Montégut, 2002; Copin-Montégut and Bégovic, 2002;
68 Touratier and Goyet, 2009) and the Otranto Strait (Krasakopoulou et al., 2011). Large
69 geographical distribution of CO₂ data are often confined to cruises with a short sampling
70 period (Álvarez et al., 2014; Goyet et al., 2015; Rivaro et al., 2010; Schneider et al., 2007;
71 Touratier et al., 2012). Numerical models have provided some insights of the carbon
72 dynamics in the Mediterranean Sea (Cossarini et al., 2015; D’Ortenzio et al., 2008; Louanchi
73 et al., 2009), but it remains important to constrain the system from in situ measurements to
74 validate their output.

75

76 The scarcity of the CO₂ system measurements in the Mediterranean Sea make it difficult to
77 constrain the CO₂ uptake in this landlocked area and also limits our understanding of the
78 magnitude and mechanisms driving the natural variability on the ocean carbon system
79 (Touratier and Goyet, 2009). Empirical modeling has been successfully used to study the
80 marine carbon biogeochemical processes such as the estimation of biologically produced O₂
81 in the mixed layer (Keeling et al., 1993), estimation of global inventories of anthropogenic
82 CO₂ (Sabine et al., 2004) and estimation of the CaCO₃ cycle (Koeve et al., 2014). Empirical
83 algorithms were also used to relate limited A_T and C_T measurements to more widely available
84 physical parameters such as salinity and temperature (Bakker et al., 1999; Ishii et al., 2004;
85 Lee et al., 2006). The A_T and C_T fields can then be used to calculate pCO₂ fields and thus
86 predict the CO₂ flux across the air-sea interface (McNeil et al., 2007).

87

88 Previous empirical approaches to constrain A_T in the Mediterranean Sea have only covered
89 selected cruises (Schneider et al., 2007; Touratier and Goyet, 2009) or local areas such as the
90 Dyfamed time-series station or the Strait of Gibraltar (Copin-Montégut, 1993; Santana-
91 Casiano et al., 2002). As for C_T, empirical models have only been applied to data below the

92 mixed layer depth (MLD) following the equation of Goyet and Davis (1997) at the Dyfamed
93 time series station (Touratier and Goyet, 2009) or using the composite dataset from Meteor
94 51/2 and Dyfamed (Touratier and Goyet, 2011). Also Lovato and Vichi (2015) proposed an
95 optimal multiple linear model for C_T using the Meteor 84/3 full water column data. To the best
96 of our knowledge the reconstruction of C_T in surface waters has not been yet performed in the
97 Mediterranean Sea. This is probably due to the lack of measurements available for previous
98 studies to capture the more complex interplay of biological, physical and solubility processes
99 that drive C_T variability in the surface waters.

100
101 In this study we have compiled CO_2 system measurements from 14 cruises between 1995 and
102 2013, that allowed us to constrain an improved and new empirical algorithms for A_T and C_T
103 in the Mediterranean Sea surface waters. We also evaluated the spatial and seasonal
104 variability of the carbon system in the Mediterranean Sea surface waters, by mapping the
105 2005-2012 annual and seasonal averages of surface A_T and C_T using the quarter degree
106 climatologies of salinity and temperature from the World Ocean Atlas 2013 (WOA13).

107 108 **2. Methods**

109 110 **2.1. Surface A_T and C_T data in the Mediterranean Sea**

111
112 Between 1998 and 2013, there have been multiple research cruises sampling the seawater
113 properties throughout the Mediterranean Sea. This includes parameters of the carbonate
114 system more specifically A_T , pH and C_T and physico-chemical properties of in situ salinity,
115 and temperature. In this study we have compiled surface water samples between 0 and 10 m
116 depth, totaling 490 and 426 measurements for A_T and C_T respectively (Table 1).

117 118 **2.2. Polynomial model for fitting A_T and C_T data**

119
120 Two polynomial equations for fitting A_T or C_T from salinity (S) alone or combined with sea
121 surface temperature (T) in the surface waters (0 – 10 m) of the Mediterranean Sea were
122 chosen from the results of the 10-fold cross validation method (Breiman, 1996; Stone, 1974).
123 This type of analysis was previously performed by Lee et al. (2006) for general relationships
124 of A_T with salinity and temperature. This model validation technique is performed by
125 randomly portioning the dataset into 10 equal subsamples. One subsample is used as the
126 validation data, and the 9 remaining subsamples are used as training data. The cross
127 validation process is then repeated 10 times, with each of the 10 subsamples used exactly
128 once as the validation data. In this manner, all observations are used both for training and
129 validation, and each observation is used for validation only once. The best fit is chosen by
130 computing the residuals from each regression model, and computing independently the
131 performance of the selected optimal polynomial on the remaining subsets.

132
133 The analysis was applied for polynomials of order 1 to 3, and the optimal equation was
134 chosen based on the lowest Root Mean Square Error (RMSE) and the highest coefficient of

135 determination (r^2). High-order polynomials (4 and above) were discarded because they can be
136 oscillatory between the data points, leading to a poorer fit to the data.

137

138 The dataset consists of 490 and 400 data points for A_T and C_T , respectively (Table 1). To
139 ensure the same spatial and temporal coverage of the polynomial fits, the same training
140 dataset was retained for both A_T and C_T . This was performed by selecting stations where both
141 parameters were simultaneously measured; yielding 360 data points (Figure 1). To validate
142 the general use of the proposed parameterizations we tested the algorithms with
143 measurements which are not included in the fits (Validation dataset). For A_T , the validation
144 dataset consists of 130 data points which are formed from the testing subset of the 10th fold
145 (40 data points), and from cruises where A_T was measured without accompanying C_T (90 data
146 points). For C_T , the validation dataset is the same as the testing subset of the 10th fold (40 data
147 points).

148

149 **2.3. Climatological and seasonal mapping of A_T and C_T**

150

151 The climatological and seasonal averages of salinity (Zweng et al., 2013) and temperature
152 (Locarnini et al., 2013) in 1/4*1/4 degree grid cells were downloaded from the World Ocean
153 Atlas 2013 (WOA13). The seven years averages (2005-2012) and the summer-winter
154 seasonality of A_T and C_T fields were mapped at 5 m depth by applying the respective derived
155 algorithms in their appropriate ranges of S and T. The summer seasonality is defined as the
156 average of the months of July, August and September. The winter seasonality is defined as
157 the average of the months of January, February, and March.

158

159 **3. Results and Discussion**

160

161 **3.1. Fitting A_T in the Mediterranean Sea surface waters**

162

163 In the surface ocean the A_T variability is controlled by freshwater addition or the effect of
164 evaporation, and salinity contributes to more than 80% of the A_T variability (Millero et al.,
165 1998). In the Mediterranean Sea, several studies have shown that the relationship between A_T
166 and S is linear (Copin-Montégut, 1993; Copin-Montégut and Bégovic, 2002; Hassoun et al.,
167 2015b; Rivaro et al., 2010; Schneider et al., 2007). In other studies, the sea surface
168 temperature (T) has been included as an additional proxy for changes in surface water A_T
169 related to convective mixing (Lee et al., 2006; Touratier and Goyet, 2011).

170

171 The results of the 10-fold cross validation analysis revealed that the optimal model for A_T is a
172 second order polynomial in which A_T is fitted to both S and T (Eq 1).

173

$$174 A_T = 2558.4 + 49.83(S - 38.2) - 3.89(T - 18) - 3.12(S - 38.2)^2 - 1.06(T - 18)^2 \quad (1)$$

175

$$175 \quad \text{Valid for } T > 13 \text{ }^\circ\text{C and } 36.30 < S < 39.65$$

176

$$176 \quad n = 375; r^2 = 0.96; RMSE = 10.6 \mu\text{mol.kg}^{-1}$$

177

178 A linear relationship between A_T and S yields a higher RMSE ($14.5 \mu\text{mol.kg}^{-1}$) and a lower r^2
179 (0.91) than Eq (1). In a semi-enclosed basin such as the Mediterranean Sea, the insulation and
180 high evaporation as well as the input of rivers and little precipitation leads to a negative
181 freshwater balance (Rohling et al., 2009). The resulting anti-estuarine thermohaline
182 circulation could explain the contribution of temperature to the A_T variability (Touratier and
183 Goyet, 2011).

184

185 The residuals of training dataset used to generate the second order polynomial fit for A_T are
186 presented in Figure 2a. Most of the A_T residuals (340 over 375) were within a range of ± 15
187 $\mu\text{mol.kg}^{-1}$ (1σ). However 35 residuals over were high up to $\pm 30 \mu\text{mol.kg}^{-1}$ (1σ). Applying
188 the A_T algorithm to the testing dataset (Figure 2b), yields a mean residual of 0.91 ± 10.30
189 $\mu\text{mol.kg}^{-1}$ (1σ), and only 6 data points have residuals higher than $\pm 15 \mu\text{mol.kg}^{-1}$ (1σ).
190 Furthermore, to make sure that the A_T algorithm does not overfit the data, we tested the
191 difference in means between the RMSE and residuals between the training set compared to
192 the testing set. The results show that for both RMSE and mean residual, we cannot reject the
193 null hypothesis (that assumes equals means) between the training and validation datasets
194 (Table 2).

195

196 The comparison of the RMSE as reported by other studies with that of Eq (1) does not
197 indicate if the parameterization developed here has advanced or not on previous attempts in
198 the Mediterranean Sea. In that order, we independently applied each of the previous
199 equations on the same training dataset used to develop Eq (1) and then computed the RMSE
200 and r^2 for every one (Table 3). The results show that Eq (1) has a lower RMSE and a higher r^2
201 than all of the parameterizations presented in Table 3. For instance, the general relationship
202 of Lee et al. (2006) applied to the dataset of this study yields an RMSE as high as ± 40.50
203 $\mu\text{mol.kg}^{-1}$. The RMSE of other studies developed strictly in the Mediterranean Sea varied
204 from ± 13.81 to $\pm 26.11 \mu\text{mol.kg}^{-1}$ using the equations of Touratier and Goyet (2011) and
205 Schneider et al. (2007) respectively.

206

207 By applying directly the previous parameterizations to our training dataset, the calculated
208 RMSE are significantly higher than the ones reported in their respective studies. For instance
209 the reported RMSE in Lee et al. (2006) for sub-tropical oceanic regions is $\pm 8 \mu\text{mol.kg}^{-1}$ and
210 that of Schneider et al. (2007) for the Meteor 51/2 cruise is $\pm 4.2 \mu\text{mol.kg}^{-1}$. This shows that
211 previous models were constrained by their spatial coverage, time span and used datasets. In
212 fact the previous equations were calculated in local areas such as the Alboran Sea (Copin-
213 Montégut, 1993), the Strait of Gibraltar (Santana-Casiano et al., 2002) or the Dyfamed Site
214 (Copin-Montégut and Bégovic, 2002; Touratier and Goyet, 2009). On a large scale, equations
215 were applied using limited datasets such as the Meteor 51/2 cruise in October-November
216 2001 (Schneider et al., 2007), the Transmed cruise in May-June 2007 (Rivaro et al., 2010) or
217 the Meteor 51/2 and the Dyfamed time series station (Touratier and Goyet, 2011).

218

219 The proposed algorithm including surface data from multiple cruises, and on a large time
220 span, presents a more representative relationship to estimate A_T from S and T than the
221 previously presented equations (Table 3). In Equation 1, T and S contribute to 96% of the A_T

222 variability and the RMSE of $\pm 10.6 \mu\text{mol.kg}^{-1}$ presents a significant improvement of the
223 spatial and temporal estimations of A_T in the Mediterranean Sea surface waters (Mean
224 difference t-test, $H = 1$; $p = 0.04$).

225

226 **3.2. Fitting C_T in the Mediterranean Sea surface waters**

227

228 The surface C_T concentrations are influenced by lateral and vertical mixing, photosynthesis,
229 oxidation of organic matter and changes in temperature and salinity (Poisson et al., 1993;
230 Takahashi et al., 1993). All these processes are directly or indirectly correlated with sea-
231 surface temperature (Lee et al., 2000). Hence, the parameterization of C_T includes both
232 physical (S and T) and/or biological parameters (Bakker et al., 1999; Bates et al., 2006; Koffi
233 et al., 2010; Lee et al., 2000; Sasse et al., 2013).

234

235 The results of the 10-fold cross validation analysis showed that a first order polynome fits C_T
236 to S and T with an RMSE of $16.25 \mu\text{mol.kg}^{-1}$ and $r^2 = 0.87$. These values are comparable to
237 the RMSE and r^2 found by previous empirical approaches applied in the Eastern Atlantic
238 (Bakker et al., 1999; Koffi et al., 2010). However we found that a third order polynome
239 improved the RMSE and r^2 of the equation compared to the first order fit (Eq 2). Hence we
240 will retain the large dataset used to develop Eq (2), where temperature and salinity explain
241 90% of the C_T variability encountered in the Mediterranean Sea surface waters. The
242 remaining 10% could be attributed to the biological and air-sea exchange contributions to the
243 C_T variability.

244

$$245 \quad C_T = 2234 + 38.15(S - 38.2) - 14.38(T - 17.7) - 4.48(S - 38.2)^2 - 1.43(S - \\ 246 \quad 38.2)(T - 17.7) + 9.62(T - 17.7)^2 - 1.10(S - 38.2)^3 + 3.53(T - 17.7)(S - 38.2)^2 + \\ 247 \quad 1.47(S - 38.2)(T - 17.7)^2 - 4.61(T - 17.7)^3 \quad (2)$$

248

$$248 \quad \text{Valid for } T > 13 \text{ }^\circ\text{C and } 36.30 < S < 39.65$$

249

$$249 \quad n = 375, r^2 = 0.90; \text{RMSE} = 14.3 \mu\text{mol.kg}^{-1}$$

250

251 The C_T parameterization developed in this study (Eq 2) showed a higher uncertainty than that
252 of A_T regarding both RMSE and r^2 . The estimation of C_T in the mixed layer adds a high
253 uncertainty due to the seasonal variability (Sabine et al., 2004). Also in the C_T are directly
254 affected by air-sea exchange, and their concentrations will increase in response to the oceanic
255 uptake of anthropogenic CO_2 .

256

257 Previous models accounted for the anthropogenic biases in the C_T measurements by
258 calculating the C_T rate of increase (Bates, 2007; Lee et al., 2000; Sasse et al., 2013;
259 Takahashi et al., 2014). However in a study, Lee et al. (2000) also did not correct the C_T
260 concentrations for regions above 30° latitude such as the Mediterranean Sea. In the following
261 we will assess the importance of accounting or not for anthropogenic biases in the C_T
262 measurements. In that order we downloaded the monthly atmospheric pCO_2 concentrations
263 measured from 1999 to 2013 at the Lampedusa Island Station (Italy) from the World Data
264 Center for Green House Gases (<http://ds.data.jma.go.jp/gmd/wdcgg/>). Following the method
265 described by Sasse et al. (2013), we corrected the C_T measurements to the nominal year of

266 2005 and applied the same 10-fold cross validation analysis using data with and without
267 anthropogenic C_T corrections. We found that the RMSE of the C_T model trained using
268 measurements with anthropogenic corrections is $13.9 \mu\text{mol.kg}^{-1}$, which is not significantly
269 different from the model trained using measurements without anthropogenic corrections (Eq
270 2; $\text{RMSE} = 14.3 \mu\text{mol.kg}^{-1}$).

271
272 The yearly increase of C_T concentrations is difficult to assess due to the wide spatial
273 distribution of the training dataset used to generate Eq (2). Hence we will refer to the monthly
274 C_T concentrations measured between 1998 and 2013 at the Dyfamed time-series station. We
275 found that the rate of increase in C_T concentrations at the Dyfamed site was $0.99 \mu\text{mol.kg}^{-1}$
276 .yr^{-1} (Figure 3), which is consistent with the anthropogenic C_T correction rate used in the
277 previous studies of Lee et al. (2000), Bates (2007) and Sasse et al. (2013).

278
279 The rate of increase in C_T concentrations of $0.99 \mu\text{mol.kg}^{-1}.\text{yr}^{-1}$ as well as the RMSE
280 difference of $\pm 0.4 \mu\text{mol.kg}^{-1}$ between the two models (with or without anthropogenic
281 corrections) are both smaller than the uncertainty of the C_T measurements of at least ± 2
282 $\mu\text{mol.kg}^{-1}$ (Millero, 2007). A recent study also showed that the uncertainty of the C_T
283 measurements can be significantly higher than $\pm 2 \mu\text{mol.kg}^{-1}$, as most laboratories reported
284 values of C_T for the measures that were within a range of $\pm 10 \mu\text{mol.kg}^{-1}$ of the stated value
285 (Bockmon and Dickson, 2015).

286
287 Between 1998 and 2013, the C_T concentrations measured at the Dyfamed time-series station
288 showed a slightly increasing trend ($r^2 = 0.05$). The increase in C_T concentrations in response
289 to elevated atmospheric CO_2 , was masked by the high seasonal variations. For example,
290 during the year 1999 the variation in C_T concentrations reached as high as $100 \mu\text{mol.kg}^{-1}$
291 (Figure 4a). Also there is a clear seasonal cycle of C_T in the Dyfamed station (Figure 4b). In
292 the summer, the C_T starts to increase gradually to reach a maximum of $2320 \mu\text{mol.kg}^{-1}$ during
293 the winter season, after which a gradual decrease is observed to reach a minimum of 2200
294 $\mu\text{mol.kg}^{-1}$ by the end of spring. The seasonal cycle can be explained by the counter effect of
295 temperature and biology on the C_T variations. During the spring, the increasing effect of
296 warming of pCO_2 is counteracted by the photosynthetic activity that lowers the C_T . During
297 the winter, the decreasing effect of cooling on pCO_2 is counteracted by the upwelling of deep
298 waters rich in C_T (Hood and Merlivat, 2001; Takahashi et al., 1993). This shows that the C_T
299 concentrations were more affected by the seasonal variations than by anthropogenic forcing.

300
301 Considering the small differences in the RMSE obtained by the two models, the uncertainties
302 in the C_T measurements and the clear signal of the seasonal variations; no corrections were
303 made to account for the rising atmospheric CO_2 concentrations. Also the dynamic
304 overturning circulation in the Mediterranean Sea plays an effective role in absorbing the
305 anthropogenic CO_2 and transports it from the surface to the interior of the basins (Hassoun et
306 al., 2015a; Lee et al., 2011).

307
308 The residuals of the dataset used to generate the third order polynomial fit for C_T are
309 presented in Figure 5a. Most of the C_T residuals (330 over 360) were within a range of ± 18

310 $\mu\text{mol.kg}^{-1}$ (1σ). In contrast only few residuals (12 over 360) reached up to $\pm 50 \mu\text{mol.kg}^{-1}$ (1
311 σ). Applying the C_T algorithm to the testing dataset (Figure 5b), yields a mean residual of 4.5
312 $\pm 17 \mu\text{mol.kg}^{-1}$ (1σ) which is close to the uncertainties of our C_T relationship. The high
313 residuals observed in this study are consistent with the results of the optimal multiple linear
314 regression performed by Lovato and Vichi (2015), where the largest discrepancies between
315 observations and reconstructed data were detected at the surface layer with RMSE higher
316 than $\pm 20 \mu\text{mol.kg}^{-1}$. To make sure that the C_T algorithm does not overfit the data, we
317 conducted the same analysis performed on the A_T datasets. The results show that for both
318 RMSE and mean residual, we cannot reject the null hypothesis (that assumes equals means)
319 between the training and validation datasets (Table 4).

320

321 Considering the high uncertainties of the C_T measurements, the seasonal variations and the
322 anthropogenic forcing; Eq (2) presents the first parametrization for C_T in the Mediterranean
323 Sea surface waters, with an RMSE of $\pm 14.3 \mu\text{mol.kg}^{-1}$ (1σ) and a $r^2 = 0.90$ (Eq 2).

324

325 **3.3. Spatial and seasonal variability of A_T and C_T in surface waters**

326

327 The ranges of the 2005-2012 average annual climatologies of the World Ocean Atlas 2013
328 (WOA13) are from 35.91 to 39.50 for S and from 16.50 °C to 23.57 °C for T (Locarnini et al.,
329 2013; Zweng et al., 2013). However a wider range is observed for the seasonal climatologies,
330 especially during the winter season where T ranges from 9.05 °C to 18.43 °C. The estimations
331 of A_T and C_T in surface waters from Eq (1) and (2) respectively are only applicable in the
332 appropriate ranges of $T > 13 \text{ °C}$ and $36.3 < S < 39.65$. Hence the surface waters A_T and C_T
333 concentrations were mapped only where T and S were within the validity range of Eq (1) and
334 (2) respectively. Excluding few near-shore areas and the influence of cold Atlantic Waters in
335 winter, the ranges in which Eq (1) and Eq (2) can be applied are within those of the
336 climatological products of T and S of the WOA13 (Figure 6).

337

338 The mapped climatologies for 2005-2012 at 5m depth show a strong increase in the Eastward
339 gradient for both A_T and C_T with the highest concentrations always found in the Eastern
340 Mediterranean (Figure 7). The minimum values of $2400 \mu\text{mol.kg}^{-1}$ for A_T and $2100 \mu\text{mol.kg}^{-1}$
341 for C_T are found near the Strait of Gibraltar and the maximum values of $2650 \mu\text{mol.kg}^{-1}$ and
342 $2300 \mu\text{mol.kg}^{-1}$ are found in the Levantine and Aegean sub-basin for A_T and C_T respectively.

343

344 The A_T parameterization of this study detects a clear signature of the alkaline waters entering
345 through the Strait of Gibraltar that remains traceable to the Strait of Sicily as also shown by
346 Cossarini et al. (2015). In the Eastern basin the positive balance between evaporation and
347 precipitation contributes to the increasing surface A_T . Local effects from some coastal areas
348 such as the Gulf of Gabes and riverine inputs from the Rhone and Po River are also detected.

349

350 Our results for surface A_T have a similar spatial pattern and range as the annual climatology
351 of Cossarini et al. (2015) which simulates surface A_T values from 2400 to $2700 \mu\text{mol.kg}^{-1}$.
352 The main difference is marked in the upper ends of the Adriatic and Aegean sub-basins
353 where our algorithm predicts A_T values around $2400\text{-}2500 \mu\text{mol.kg}^{-1}$, whereas the analysis of

354 Cossarini et al. (2015) yields a maximum of $2700 \mu\text{mol.kg}^{-1}$ in these regions. Regressions in
355 regions of river input indicate a negative correlation between alkalinity and salinity (Luchetta
356 et al., 2010). Hence, Eastern marginal seas such as the Adriatic and Aegean sub-basins have
357 high A_T concentrations due to the freshwater inputs (Cantoni et al., 2012; Souvermezoglou et
358 al., 2010). This shows the sensitivity of our algorithms to temperature and salinity especially
359 in areas that are more influenced by continental inputs such as the Po River and inputs of the
360 Dardanelle in the northern Adriatic and northern Aegean respectively (Figure 7a).

361
362 At the surface, the basin wide distributions of C_T are affected by physical processes and their
363 gradient is similar to that of A_T (Figure 7b). The lowest C_T concentrations are found in the
364 zone of the inflowing Atlantic water and increases toward the East in part due to evaporation
365 as also shown by Schneider et al. (2010). Our results for surface C_T have a similar range as
366 the optimal linear regression performed by Lovato and Vichi (2015) which estimates surface
367 C_T values from 2180 to $2260 \mu\text{mol.kg}^{-1}$. Moreover, the results show that the Mediterranean
368 Sea is characterized by C_T values that are much higher ($100\text{--}200 \mu\text{mol.kg}^{-1}$ higher) than
369 those observed in the Atlantic Ocean at the same latitude (Key et al., 2004).

370
371 Overall the Western basin has a lower surface C_T content than the Eastern basin which could
372 be explained by the Eastward decrease of the Mediterranean Sea trophic gradient (Lazzari et
373 al., 2012). The higher rate of inorganic carbon consumption by photosynthesis in the Western
374 basin can lead to the depletion of C_T in the surface waters, whereas the ultra-oligotrophic
375 state in the Eastern basin can lead to a high remineralization rate that consumes oxygen and
376 enriches surface waters with C_T (Moutin and Raimbault, 2002).

377
378 The magnitude of the seasonal variability between summer and winter for A_T and C_T is
379 shown in Figure 8. Unlike the seven years averages, the seasonal climatological variations
380 (2005-2012) of A_T have different spatial patterns than those of C_T . Overall the summer-
381 winter time differences for A_T have an increasing Eastward gradient (Figure 8a). The largest
382 magnitudes are marked in the Alboran Sea with differences reaching up to $-80 \mu\text{mol.kg}^{-1}$; the
383 negative difference implies that during the winter inflowing surface Atlantic water has higher
384 A_T concentrations than in summer. Higher winter than summer time A_T concentrations are
385 also observed in the Balearic, Ligurian and the South-Western Ionian sub-basins but with a
386 less pronounced seasonality ($\sim -30 \mu\text{mol.kg}^{-1}$). For these three sub-basins, the C_T has a higher
387 summer-winter magnitude than A_T ($\sim -70 \mu\text{mol.kg}^{-1}$). The winter cooling of surface waters
388 increases their density and promotes a mixing with deeper water. Thus, the enrichment in
389 winter time likely reflects the upwelling of deep waters that have accumulated A_T and C_T
390 from the remineralization of organic matter, respiration and the dissolution of CaCO_3 . The
391 seasonality is more pronounced for C_T , which likely reflects the stronger response of C_T to
392 biological processes than A_T (Takahashi et al., 1993).

393
394 In the Algerian sub-basin and along the coasts of Tunisia and Libya, the seasonality is
395 inversed with higher A_T and C_T concentrations prevailing in the summer. The African coast is
396 an area of coastal downwelling during the winter season. However, during summer the
397 coastal upwelling appears in response to turning of the wind near the coast toward the West

398 (Bakun and Agostini, 2001). In general, the magnitude of the A_T seasonal variability is higher
399 in summer than in winter for the Eastern basin and more particularly in the Ionian and
400 Levantine sub-basins. During this season strong evaporation takes place and induce an
401 increase of A_T concentrations (Schneider et al., 2007). In the Eastern basin, the high
402 evaporation during the summer has a smaller effect on the C_T , and magnitudes reach their
403 maxima in the Levantine sub-basin ($\sim + 20 \mu\text{mol.kg}^{-1}$). During winter time the Western basin
404 and South East of Sicily appear to be dominated by higher C_T concentrations than the rest of
405 the Eastern basin, where the summer C_T concentrations are prevailing (Figure 8b). During
406 winter the high C_T concentrations that coincide with low SST in the Western basin, could
407 result from the deepening of the mixed layer and could be enhanced by the upwelling
408 associated with the Tramontane-Mistral winds that blow from the southern of France and
409 reach the Balearic Islands and the Spanish coast.

410

411 **Summary**

412

413 The A_T and C_T algorithms are derived from a compilation of 490 and 426 quality controlled
414 surface measurements respectively, collected between 1999 and 2013 in the Mediterranean
415 Sea. A second order polynomial relating A_T to both S and T yielded a lower RMSE (± 10.4
416 $\mu\text{mol.kg}^{-1}$) and a higher r^2 (0.96) than a linear fit deriving A_T from S alone. This confirmed
417 the important contribution of temperature to the A_T variability. Hence, temperature should be
418 included in future algorithms to help better constrain the surface A_T variations. The proposed
419 second order polynomial had a lower RMSE than other studies when we applied their
420 respective algorithms to the same training dataset. In this study we propose an improved and
421 more global relationship to estimate the A_T spatial and temporal variations in the
422 Mediterranean Sea surface waters.

423

424 The C_T parameterization is a first attempt to estimate the surface variations in the
425 Mediterranean Sea. A third order polynomial is suggested to fit the C_T to T and S with a
426 RMSE of $\pm 14.3 \mu\text{mol.kg}^{-1}$. The biological contributions to the C_T variations were less
427 pronounced than the physical processes. The contributions of to the physical processes and
428 biology to the C_T variability were 90 and 10 % respectively. In terms of anthropogenic
429 forcing, the C_T rate of increase of $0.99 \mu\text{mol.kg}^{-1}.\text{yr}^{-1}$ was significantly lower than the
430 uncertainty of the measurements than can reach $\pm 10 \mu\text{mol.kg}^{-1}$ between different
431 laboratories. Moreover the C_T concentrations were more affected by the seasonal variations
432 than the increase of atmospheric CO_2 .

433

434 We propose to use Equations (1) and (2) for the estimation of surface A_T and C_T in the
435 Mediterranean Sea when salinity and temperature of the area are available and are in the
436 appropriate ranges of the equations. However in the Eastern marginal seas especially the
437 northern Adriatic and northern Aegean there is a need to develop a more specific equation
438 that minimizes the errors in these areas. Hence, it is important to enrich the existing dataset
439 by an extensive sampling program such as the Med-SHIP initiative (CIESM, 2012) in order
440 to improve the modeling of the carbonate system over the whole Mediterranean Sea.

441

442
443
444
445
446
447
448
449
450
451
452
453
454
455
456
457
458
459
460
461
462
463
464
465
466
467
468
469
470
471
472
473
474
475
476
477
478
479
480
481
482
483
484
485
486
487

Acknowledgments

The authors would like to thank all parties that have contributed to the data provision in particular:

- The Sesame IT4 and Moose-GE cruise data were provided through SeaDataNet - Pan-European infrastructure for ocean and marine data management (<http://www.seadatanet.org>).
 - The DYFAMED time series have been provided by the Oceanological Observatory of Villefranche-sur-Mer (L.Coppola). This project is funded by CNRS-INSU and ALLENVI through the MOOSE observing network".
 - The Transmed cruise data were provided by Dr. Rivaro, P., Dr. Russo, A. and Dr. Kovacevic, V. The Transmed cruise is part of the VECTOR Project, funded by: the Ministry of Education, University and Research, the Ministry of Economy and Finance, the Ministry of the Environment and Protection of Natural Resources and the Ministry of Agriculture and Forestry with an Integrated Special Fund for Research (FISR).
 - The MedSEA 2013 cruise data were provided by the University of Perpignan Via Domitia: 'Institut de Modélisation et d'Analyse en Géo-Environnements et Santé, ESPACE-DEV' (Goyet, C. and Hassoun, A.E.R.). This project was funded by the EC "Mediterranean Sea Acidification in a changing climate" project (MedSeA; grant agreement 265103).
 - We would like also to thank the SNAPO-CO₂ (Service National d'Analyse des paramètres Océaniques du CO₂) for their contribution in measuring some of the A_T and C_T samples.
- Authors are also grateful to the National Council for Scientific Research (CNRS) in Lebanon for the PhD thesis scholarship granted to Miss Gemayel Elissar.

References

- Álvarez, M., Sanleón-Bartolomé, H., Tanhua, T., Mintrop, L., Luchetta, A., Cantoni, C., Schroeder, K., and Civitarese, G.: The CO₂ system in the Mediterranean Sea: a basin wide perspective, *Ocean Sci*, 10, 69-92, 2014.
- Bakker, D. C. E., de Baar, H. J. W., and de Jong, E.: The dependence on temperature and salinity of dissolved inorganic carbon in East Atlantic surface waters, *Mar Chem*, 65, 263-280, 1999.
- Bakun, A. and Agostini, V. N.: Seasonal patterns of wind-induced upwelling/downwelling in the Mediterranean Sea, *Sci Mar*, 65, 243-257, 2001.
- Bates, N. R.: Interannual variability of the oceanic CO₂ sink in the subtropical gyre of the North Atlantic Ocean over the last 2 decades, *J Geophys Res*, 112, C09013, 2007.
- Bates, N. R., Pequignet, A. C., and Sabine, C. L.: Ocean carbon cycling in the Indian Ocean: 1. Spatiotemporal variability of inorganic carbon and air-sea CO₂ gas exchange, *Global Biogeochem Cycles*, 20, GB3020, 2006.
- Bégovic, M. and Copin-Montégut, C.: Processes controlling annual variations in the partial pressure of CO₂ in surface waters of the central northwestern Mediterranean Sea (Dyfamed site), *Deep Sea Res. Part II Top Stud Oceanogr*, 49, 2031-2047, 2002.
- Bégovic, M. and Copin, C.: Alkalinity and pH measurements on water bottle samples during THALASSA cruise PROSOPE. 2013.

488 Bockmon, E. E. and Dickson, A. G.: An inter-laboratory comparison assessing the quality of
489 seawater carbon dioxide measurements, *Mar Chem*, 171, 36-43, 2015.

490 Breiman, L.: Stacked regressions, *Mach Learn*, 24, 49-64, 1996.

491 Cantoni, C., Luchetta, A., Celio, M., Cozzi, S., Raicich, F., and Catalano, G.: Carbonate
492 system variability in the Gulf of Trieste (North Adriatic Sea), *Estuar Coast Shelf Sci*,
493 115, 51-62, 2012.

494 CIESM: Designing Med-SHIP: a Program for repeated oceanographic surveys, CIESM,
495 Monaco, 164 pp., 2012.

496 Copin-Montégut, C.: Alkalinity and carbon budgets in the Mediterranean Sea, *Global*
497 *Biogeochem Cycles*, 7, 915-925, 1993.

498 Copin-Montégut, C. and Bégovic, M.: Distributions of carbonate properties and oxygen along
499 the water column (0–2000m) in the central part of the NW Mediterranean Sea
500 (Dyfamed site): influence of winter vertical mixing on air–sea CO₂ and O₂ exchanges,
501 *Deep Sea Res. Part II Top Stud Oceanogr*, 49, 2049-2066, 2002.

502 Cossarini, G., Lazzari, P., and Solidoro, C.: Spatiotemporal variability of alkalinity in the
503 Mediterranean Sea, *Biogeosciences*, 12, 1647-1658, 2015.

504 D’Ortenzio, F., Antoine, D., and Marullo, S.: Satellite-driven modeling of the upper ocean
505 mixed layer and air–sea CO₂ flux in the Mediterranean Sea, *Deep Sea Res. Part I*
506 *Oceanogr Res Pap*, 55, 405-434, 2008.

507 Goyet, C. and Davis, D.: Estimation of total CO₂ concentration throughout the water column,
508 *Deep Sea Res. Part I Oceanogr Res Pap*, 44, 859-877, 1997.

509 Goyet, C., Hassoun, A. E. R., and Gemayel, E.: Carbonate system during the May 2013
510 MedSeA cruise. *Pangaea*, 2015.

511 Hassoun, A. E. R., Gemayel, E., Krasakopoulou, E., Goyet, C., Abboud-Abi Saab, M.,
512 Guglielmi, V., Touratier, F., and Falco, C.: Acidification of the Mediterranean Sea from
513 anthropogenic carbon penetration, *Deep Sea Res. Part I Oceanogr Res Pap*, 102, 1-15,
514 2015a.

515 Hassoun, A. E. R., Gemayel, E., Krasakopoulou, E., Goyet, C., Abboud-Abi Saab, M., Ziveri,
516 P., Touratier, F., Guglielmi, V., and Falco, C.: Modeling of the total alkalinity and the
517 total inorganic carbon in the Mediterranean Sea, *J Water Resource Ocean Sci*, 4, 24-32,
518 2015b.

519 Hood, E. M. and Merlivat, L.: Annual to interannual variations of fCO₂ in the northwestern
520 Mediterranean Sea: Results from hourly measurements made by CARIOCA buoys,
521 1995-1997, *J Mar Res*, 59, 113-131., 2001.

522 Huertas, E.: Hydrochemistry measured on water bottle samples during Al Amir Moulay
523 Abdallah cruise CARBOGIB-2. Unidad de Tecnología Marina - Consejo Superior de
524 Investigaciones Científicas, 2007a.

525 Huertas, E.: Hydrochemistry measured on water bottle samples during Al Amir Moulay
526 Abdallah cruise CARBOGIB-3. Unidad de Tecnología Marina - Consejo Superior de
527 Investigaciones Científicas, 2007b.

528 Huertas, E.: Hydrochemistry measured on water bottle samples during Al Amir Moulay
529 Abdallah cruise CARBOGIB-4. Unidad de Tecnología Marina - Consejo Superior de
530 Investigaciones Científicas, 2007c.

531 Huertas, E.: Hydrochemistry measured on water bottle samples during Al Amir Moulay
532 Abdallah cruise CARBOGIB-5. Unidad de Tecnología Marina - Consejo Superior de
533 Investigaciones Científicas, 2007d.

534 Huertas, E.: Hydrochemistry measured on water bottle samples during Al Amir Moulay
535 Abdallah cruise CARBOGIB-6. Unidad de Tecnología Marina - Consejo Superior de
536 Investigaciones Científicas, 2007e.

537 Huertas, E.: Hydrochemistry measured on water bottle samples during Garcia del Cid cruise
538 GIFT-1. Unidad de Tecnología Marina - Consejo Superior de Investigaciones
539 Científicas, 2007f.

540 Huertas, E.: Hydrochemistry measured on water bottle samples during Garcia del Cid cruise
541 GIFT-2. Unidad de Tecnología Marina - Consejo Superior de Investigaciones
542 Científicas, 2007g.

543 Huertas, E.: Hydrochemistry measured on water bottle samples during Garcia del Cid cruise
544 GIFT-3. Unidad de Tecnología Marina - Consejo Superior de Investigaciones
545 Científicas, 2007h.

546 Hydes, D., Jiang, Z., Hartman, M. C., Campbell, J. M., Hartman, S. E., Pagnani, M. R., and
547 Kelly-Gerreyn, B. A.: Surface DIC and TALK measurements along the M/V Pacific
548 Celebes VOS Line during the 2007-2012 cruises.
549 http://cdiac.ornl.gov/ftp/oceans/VOS_Pacific_Celebes_line/. Carbon Dioxide
550 Information Analysis Center, Oak Ridge National Laboratory, US Department of
551 Energy, Oak Ridge, Tennessee. doi: 10.3334/CDIAC/OTG.VOS_PC_2007-2012, 2012.

552 Ishii, M., Saito, S., Tokieda, T., Kawano, T., Matsumoto, K., and Inoue, H. Y.: Variability of
553 surface layer CO₂ parameters in the Western and Central Equatorial Pacific. In: Global
554 Environmental Change in the Ocean and on Land, Shiyomi M., K. H., Koizumi H.,
555 Tsuda A., Awaya Y. (Ed.), TERRAPUB, Tokyo, 2004.

556 Keeling, R. F., Najjar, R. P., Bender, M. L., and Tans, P. P.: What atmospheric oxygen
557 measurements can tell us about the global carbon cycle, *Global Biogeochem Cycles*, 7,
558 37-67, 1993.

559 Key, R. M., Kozyr, A., Sabine, C. L., Lee, K., Wanninkhof, R., Bullister, J. L., Feely, R. A.,
560 Millero, F. J., Mordy, C., and Peng, T. H.: A global ocean carbon climatology: Results
561 from Global Data Analysis Project (GLODAP), *Global Biogeochem Cycles*, 18,
562 GB4031, 2004.

563 Koeve, W., Duteil, O., Oschlies, A., Kähler, P., and Segschneider, J.: Methods to evaluate
564 CaCO₃ cycle modules in coupled global biogeochemical ocean models, *Geosci Model*
565 *Dev*, 7, 2393-2408, 2014.

566 Koffi, U., Lefèvre, N., Kouadio, G., and Boutin, J.: Surface CO₂ parameters and air-sea CO₂
567 flux distribution in the Eastern Equatorial Atlantic Ocean, *J Mar Syst*, 82, 135-144,
568 2010.

569 Krasakopoulou, E., Souvermezoglou, E., and Goyet, C.: Anthropogenic CO₂ fluxes in the
570 Otranto Strait (E. Mediterranean) in February 1995, *Deep Sea Res. Part I Oceanogr Res*
571 *Pap*, 58, 1103-1114, 2011.

572 Lazzari, P., Solidoro, C., Ibello, V., Salon, S., Teruzzi, A., Béranger, K., Colella, S., and
573 Crise, A.: Seasonal and inter-annual variability of plankton chlorophyll and primary
574 production in the Mediterranean Sea: a modelling approach, *Biogeosciences*, 9, 217-
575 233, 2012.

576 Lee, K., Sabine, C. L., Tanhua, T., Kim, T.-W., Feely, R. A., and Kim, H.-C.: Roles of
577 marginal seas in absorbing and storing fossil fuel CO₂, *Energy Environ Sci*, 4, 1133-
578 1146, 2011.

579 Lee, K., Tong, L. T., Millero, F. J., Sabine, C. L., Dickson, A. G., Goyet, C., Park, G.-H.,
580 Wanninkhof, R., Feely, R. A., and Key, R. M.: Global relationships of total alkalinity
581 with salinity and temperature in surface waters of the world's oceans, *Geophys Res Lett*,
582 33, L19605, 2006.

583 Lee, K., Wanninkhof, R., Feely, R. A., Millero, F. J., and Peng, T.-H.: Global relationships of
584 total inorganic carbon with temperature and nitrate in surface seawater, *Global*
585 *Biogeochem Cycles*, 14, 979-994, 2000.

586 Locarnini, R. A., Mishonov, A. V., Antonov, J. I., Boyer, T. P., Garcia, H. E., Baranova, O.
587 K., Zweng, M. M., Paver, C. R., Reagan, J. R., Johnson, D. R., Hamilton, M., and
588 Seidov, D.: World Ocean Atlas 2013, Volume 1: Temperature, NOAA Atlas NESDIS
589 73, 40 pp., 2013.

590 Louanchi, F., Boudjakdji, M., and Nacef, L.: Decadal changes in surface carbon dioxide and
591 related variables in the Mediterranean Sea as inferred from a coupled data-diagnostic
592 model approach, *ICES J Mar Sci*, 66, 1538-1546, 2009.

593 Lovato, T. and Vichi, M.: An objective reconstruction of the Mediterranean sea carbonate
594 system, *Deep Sea Res. Part I Oceanogr Res Pap*, 98, 21-30, 2015.

595 Luchetta, A., Cantoni, C., and Catalano, G.: New observations of CO₂ induced acidification
596 in the northern Adriatic Sea over the last quarter century, *Chem Ecol*, 26, 1-17, 2010.

597 McNeil, B. I., Metzl, N., Key, R. M., Matear, R. J., and Corbiere, A.: An empirical estimate
598 of the Southern Ocean air-sea CO₂ flux, *Global Biogeochem Cycles*, 21, GB3011, 2007.

599 Medar-Group: MEDATLAS 2002. Mediterranean and Black Sea database of temperature,
600 salinity and biochemical parameters. Climatological Atlas., 2002.

601 Millero, F. J.: The Marine inorganic carbon cycle, *Chem Rev*, 107, 308-341, 2007.

602 Millero, F. J., Lee, K., and Roche, M.: Distribution of alkalinity in the surface waters of the
603 major oceans, *Mar Chem*, 60, 111-130, 1998.

604 Moutin, T. and Raimbault, P.: Primary production, carbon export and nutrients availability in
605 Western and Eastern Mediterranean Sea in early summer 1996 (MINOS cruise), *J Mar*
606 *Syst*, 33–34, 273-288, 2002.

607 Omta, A. W., Dutkiewicz, S., and Follows, M. J.: Dependence of the ocean-atmosphere
608 partitioning of carbon on temperature and alkalinity, *Global Biogeochem Cycles*, 25,
609 GB1003, 2011.

610 Perez, F. F., Rios, A. F., Pelegri, J. L., de la Paz, M., Alonso, F., Royo, E., Velo, A., Garcia-
611 Ibanez, M., and Padin, X. A.: Carbon Data Obtained During the R/V Hesperides Cruise
612 in the Atlantic Ocean on CLIVAR Repeat Hydrography Section A17, FICARAM XV,
613 (March 20 - May 2, 2013).
614 http://cdiac.ornl.gov/ftp/oceans/CLIVAR/A17_FICARAM_XV_2013/. Carbon Dioxide
615 Information Analysis Center, Oak Ridge National Laboratory, US Department of
616 Energy, Oak Ridge, Tennessee. doi: 10.3334/CDIAC/OTG.CLIVAR_FICARAM_XV
617 2013.

618 Poisson, A., Metzl, N., Brunet, C., Schauer, B., Bres, B., Ruiz-Pino, D., and Louanchi, F.:
619 Variability of sources and sinks of CO₂ in the western Indian and southern oceans
620 during the year 1991, *J Geophys Res*, 98, 22759-22778, 1993.

621 Rivaro, P., Messa, R., Massolo, S., and Frache, R.: Distributions of carbonate properties
622 along the water column in the Mediterranean Sea: Spatial and temporal variations, *Mar*
623 *Chem*, 121, 236-245, 2010.

624 Rödenbeck, C., Keeling, R. F., Bakker, D. C. E., Metzl, N., Olsen, A., Sabine, C., and
625 Heimann, M.: Global surface-ocean pCO₂ and sea-air CO₂ flux variability from an
626 observation-driven ocean mixed-layer scheme, *Ocean Sci*, 9, 193-216, 2013.

627 Rohling, E. J., Abu-Zied, R. H., Casford, J. S. L., Hayes, A., and Hoogakker, B. A. A.: The
628 marine environment: Present and past. In: *The physical geography of the*
629 *Mediterranean*, Woodward, J. C. (Ed.), Oxford University Press, 2009.

630 Sabine, C. L., Feely, R. A., Gruber, N., Key, R. M., Lee, K., Bullister, J. L., Wanninkhof, R.,
631 Wong, C. S., Wallace, D. W. R., Tilbrook, B., Millero, F. J., Peng, T.-H., Kozyr, A.,
632 Ono, T., and Rios, A. F.: The oceanic sink for anthropogenic CO₂, *Science*, 305, 367-
633 371, 2004.

634 Santana-Casiano, J. M., Gonzalez-Davila, M., and Laglera, L. M.: The carbon dioxide system
635 in the Strait of Gibraltar, *Deep Sea Res. Part II Top Stud Oceanogr*, 49, 4145-4161,
636 2002.

637 Sasse, T. P., McNeil, B. I., and Abramowitz, G.: A novel method for diagnosing seasonal to
638 inter-annual surface ocean carbon dynamics from bottle data using neural networks,
639 *Biogeosciences*, 10, 4319-4340, 2013.

640 Schneider, A., Tanhua, T., Körtzinger, A., and Wallace, D. W. R.: High anthropogenic
641 carbon content in the Eastern Mediterranean, *J Geophys Res*, 115, C12050, 2010.

642 Schneider, A., Wallace, D. W. R., and Körtzinger, A.: Alkalinity of the Mediterranean Sea,
643 *Geophys Res Lett*, 34, L15608, 2007.

644 Schneider, B. and Roether, W.: Meteor 06MT20011018 cruise data from the 2001 cruises,
645 CARINA Data Set. <http://cdiac.ornl.gov/ftp/oceans/CARINA/Meteor/06MT512/>.
646 Carbon Dioxide Information Analysis Center, Oak Ridge National Laboratory, US
647 Department of Energy, Oak Ridge, Tennessee. doi: 10.3334/CDIAC/otg.CARINA
648 06MT20011018, 2007.

649 Souvermezoglou, E., Krasakopoulou, E., and Goyet, C.: Total inorganic carbon and total
650 alkalinity distribution in the Aegean Sea, *CIESM*, 312 pp., 2010.

651 Stone, M.: Cross validatory choice and assessment of statistical predictions, *J R Stat Soc*
652 *Series B Stat Methodol*, 36, 111-147, 1974.

653 Takahashi, T., Olafsson, J., Goddard, J. G., Chipman, D. W., and Sutherland, S. C.: Seasonal
654 variation of CO₂ and nutrients in the high-latitude surface oceans: A comparative study,
655 *Global Biogeochem Cycles*, 7, 843-878, 1993.

656 Takahashi, T., Sutherland, S. C., Chipman, D. W., Goddard, J. G., Ho, C., Newberger, T.,
657 Sweeney, C., and Munro, D. R.: Climatological distributions of pH, pCO₂, total CO₂,
658 alkalinity, and CaCO₃ saturation in the global surface ocean, and temporal changes at
659 selected locations, *Mar Chem*, 164, 95-125, 2014.

660 Takahashi, T., Sutherland, S. C., Wanninkhof, R., Sweeney, C., Feely, R. A., Chipman, D.
661 W., Hales, B., Friederich, G., Chavez, F., Sabine, C., Watson, A., Bakker, D. C. E.,
662 Schuster, U., Metzl, N., Yoshikawa-Inoue, H., Ishii, M., Midorikawa, T., Nojiri, Y.,
663 Körtzinger, A., Steinhoff, T., Hoppema, M., Olafsson, J., Arnarson, T. S., Tilbrook, B.,
664 Johannessen, T., Olsen, A., Bellerby, R., Wong, C. S., Delille, B., Bates, N. R., and de
665 Baar, H. J. W.: Climatological mean and decadal change in surface ocean pCO₂, and net
666 sea-air CO₂ flux over the global oceans, *Deep Sea Res. Part II Top Stud Oceanogr*, 56,
667 554-577, 2009.

668 Tanhua, T., Alvarez, M., and Mintrop, L.: Carbon dioxide, hydrographic, and chemical data
669 obtained during the R/V Meteor MT84_3 Mediterranean Sea cruise (April 5. - April 28,
670 2011). http://cdiac.ornl.gov/ftp/oceans/CLIVAR/Met_84_3_Med_Sea/. Carbon Dioxide
671 Information Analysis Center, Oak Ridge National Laboratory, US Department of
672 Energy, Oak Ridge, Tennessee. doi: 10.3334/CDIAC/OTG.CLIVAR_06MT20110405,
673 2012.

674 Touratier, F. and Goyet, C.: Decadal evolution of anthropogenic CO₂ in the northwestern
675 Mediterranean Sea from the mid-1990s to the mid-2000s, *Deep Sea Res. Part I*
676 *Oceanogr Res Pap*, 56, 1708-1716, 2009.

677 Touratier, F. and Goyet, C.: Impact of the Eastern Mediterranean Transient on the
678 distribution of anthropogenic CO₂ and first estimate of acidification for the
679 Mediterranean Sea, *Deep Sea Res. Part I Oceanogr Res Pap*, 58, 1-15, 2011.

680 Touratier, F., Guglielmi, V., Goyet, C., Prieur, L., Pujo-Pay, M., Conan, P., and Falco, C.:
681 Distributions of the carbonate system properties, anthropogenic CO₂, and acidification
682 during the 2008 BOUM cruise (Mediterranean Sea), *Biogeosci Discuss*, 9, 2709-2753,
683 2012.

684 Wanninkhof, R., Park, G. H., Takahashi, T., Sweeney, C., Feely, R., Nojiri, Y., Gruber, N.,
685 Doney, S. C., McKinley, G. A., Lenton, A., Le Quéré, C., Heinze, C., Schwinger, J.,
686 Graven, H., and Khatiwala, S.: Global ocean carbon uptake: magnitude, variability and
687 trends, *Biogeosciences*, 10, 1983-2000, 2013.

688 Watson, A. and Orr, J.: Carbon Dioxide Fluxes in the Global Ocean. In: *Ocean*
689 *Biogeochemistry*, Fasham, M. R. (Ed.), *Global Change — The IGBP Series (closed)*,
690 Springer Berlin Heidelberg, 2003.

691 Zweng, M. M., Reagan, J. R., Antonov, J. I., Locarnini, R. A., Mishonov, A. V., Boyer, T. P.,
692 Garcia, H. E., Baranova, O. K., Johnson, D. R., Seidov, D., and Biddle, M. M.: *World*
693 *Ocean Atlas 2013, Volume 2: Salinity*. Levitus, S., Ed. and Mishonov, A., Technical Ed
694 (Eds.), NOAA Atlas NESDIS 74, 2013.

695
696
697
698
699
700
701
702
703
704
705
706
707
708
709
710
711
712
713
714
715
716
717
718
719
720
721
722
723
724
725
726
727
728

729
730
731
732

Table 1. List of available carbonate system datasets for the Mediterranean Sea

Dataset	Period	Area	Carbonate system parameters	Data points	Reference
Prosope	Sep-Oct 1999	Mediterranean Sea	A_T and pH	20	Bégovic and Copin (2013)
Meteor 51/2	Oct-Nov 2001	Eastern Mediterranean	A_T and C_T	16	Schneider and Roether (2007)
Meteor 84/3	Apr 2004	Southern Mediterranean	A_T , C_T and pH	16	Tanhua et al. (2012)
Carbogib 2-6	2005-2006	Gibraltar Strait	A_T and pH	28	(Huertas, 2007a, b, c, d, e)
Gift 1-3	2005-2006	Gibraltar Strait	A_T and pH	12	(Huertas, 2007f, g, h)
Transmed	Jun 2007	Eastern Mediterranean	A_T and pH	20	Rivaro et al. (2010)
Sesame IT-4	Mar - Apr 2008	Northern Mediterranean	A_T and C_T	16	SeaDataNet
Boum	Jun-Jul 2008	Mediterranean Sea	A_T and C_T	75	Touratier et al. (2012)
Pacific-Celebes	2007-2009	Mediterranean Sea	A_T and C_T	22	Hydes et al. (2012)
Moose-GE	May 2010	Ligurian Sea	A_T and C_T	44	SeaDataNet
Hesperides	May 2013	Gibraltar Strait	A_T	10	Perez et al. (2013)
MedSeA	May 2013	Southern Mediterranean	A_T and C_T	59	Goyet et al. (2015)
Dyfamed time-series	1998-2013	Ligurian Sea	A_T and C_T	152	Oceanological Observatory of Villefranche-sur-Mer

733
734
735
736
737
738
739
740
741
742
743
744
745

746
747
748
749
750

Table 2. Mean difference t-test for the A_T algorithm between the training and validation datasets

	Training dataset	Validation dataset	
RMSE ($\mu\text{mol.kg}^{-1}$)	10.60	10.34	Mean difference t-test: H = 0; p = 0.83
Mean residual ($\mu\text{mol.kg}^{-1}$)	$2.64\text{e-}13 \pm 10.57$	0.91 ± 10.30	Mean difference t-test: H = 0; p = 0.42

751
752
753
754
755
756
757
758
759
760
761
762
763
764
765
766
767
768
769
770
771
772
773
774
775
776
777
778
779
780
781
782
783
784

785
786
787
788
789

Table 3. Performance of the different parameterizations for the estimation of A_T applied independently to the training dataset of this study

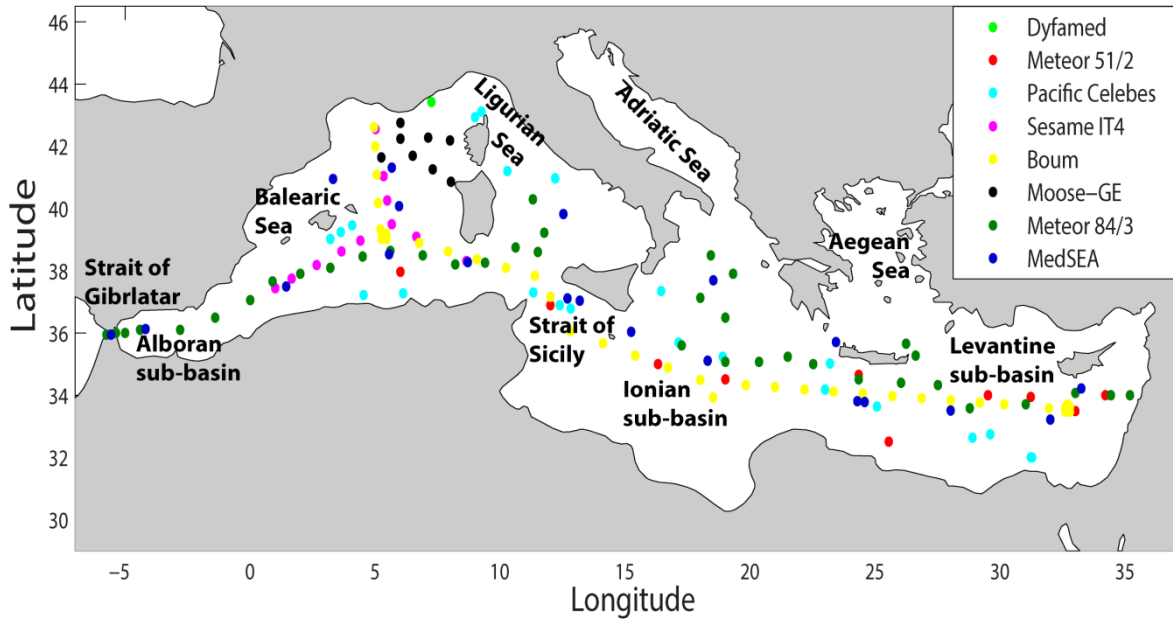
Region	Parameterization	RMSE ($\mu\text{mol.kg}^{-1}$)	r^2	Reference
Alboran Sea	$A_T = 94.85(S) - 1072.6$	± 16.61	0.92	Copin-Montégut (1993)
Dyfamed site	$A_T = 93.99(S) - 1038.1$	± 16.31	0.92	Copin-Montégut and Bégovic (2002)
Strait of Gibraltar	$A_T = 92.28(S) - 968.7$	± 16.48	0.92	Santana-Casiano et al. (2002)
Mediterranean Sea	$A_T = 73.7(S) - 285.7$	± 26.11	0.68	Schneider et al. (2007)
Dyfamed site	$A_T = 99.26(S) - 1238.4$	± 18.53	0.91	Touratier and Goyet (2009)
Western Mediterranean	$A_T = 95.25(S) - 1089.3$	± 16.97	0.92	Rivaro et al. (2010)
Eastern Mediterranean	$A_T = 80.04(S) - 499.8$	± 14.58	0.91	
Mediterranean Sea	$A_T = 1/(6.57 \cdot 10^{-5} + 1.77 \cdot 10^{-2})/S - (5.93 - 10^{-4}(\ln\theta))/\theta^2$	± 13.81	0.92	Touratier and Goyet (2011)
Global relationship (Sub-tropics)	$A_T = 2305 + 58.66 (S - 35) + 2.32 (S - 35)^2 + 1.41 (T - 20) + 0.04 (T - 20)^2$	± 40.50	0.26	Lee et al. (2006)

790
791
792
793
794
795
796
797
798
799
800
801
802
803
804
805
806

807
808
809
810
811
812
813
814
815
816
817
818
819
820
821
822
823
824
825
826
827
828
829
830
831
832
833
834
835
836
837
838
839
840
841
842
843

Table 4. Mean difference t-test for the C_T algorithm between the training and validation datasets

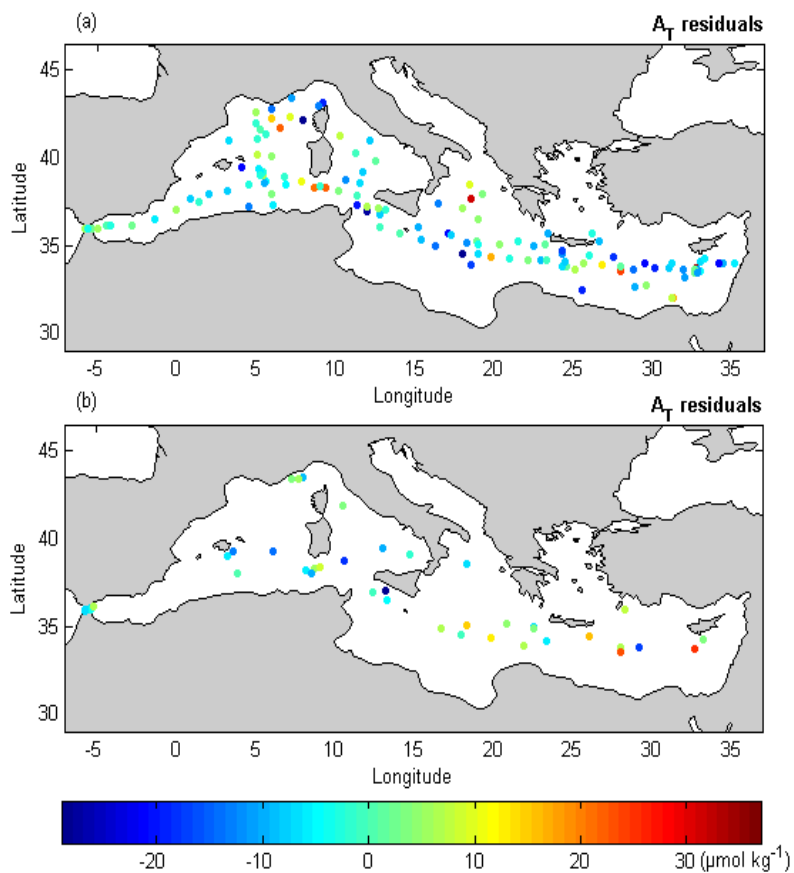
	Training dataset	Validation dataset	
RMSE ($\mu\text{mol.kg}^{-1}$)	14.3	16.2	Mean difference t-test: $H = 0$; $p = 0.04$
Mean residual ($\mu\text{mol.kg}^{-1}$)	$-1.5\text{e-}12 \pm 14.2$	4.5 ± 17	Mean difference t-test: $H = 0$; $p = 0.06$



844 **Figure 1. Spatial distribution of data points used to initiate the fits of A_T and C_T**

845
846
847
848
849
850
851
852
853
854
855
856
857
858
859
860
861
862
863
864
865
866
867
868
869
870
871
872

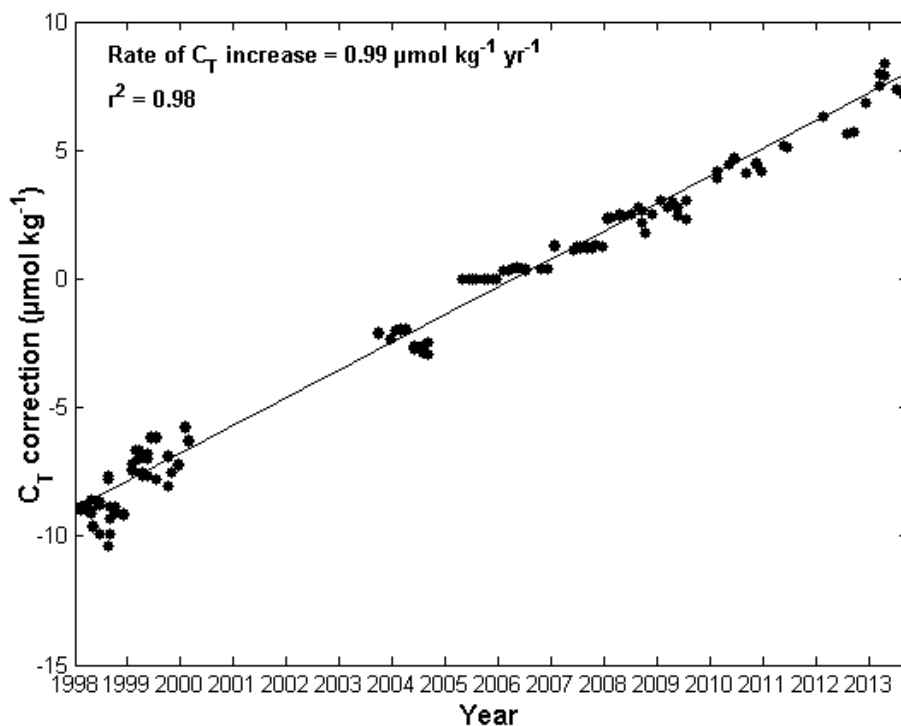
873
874
875



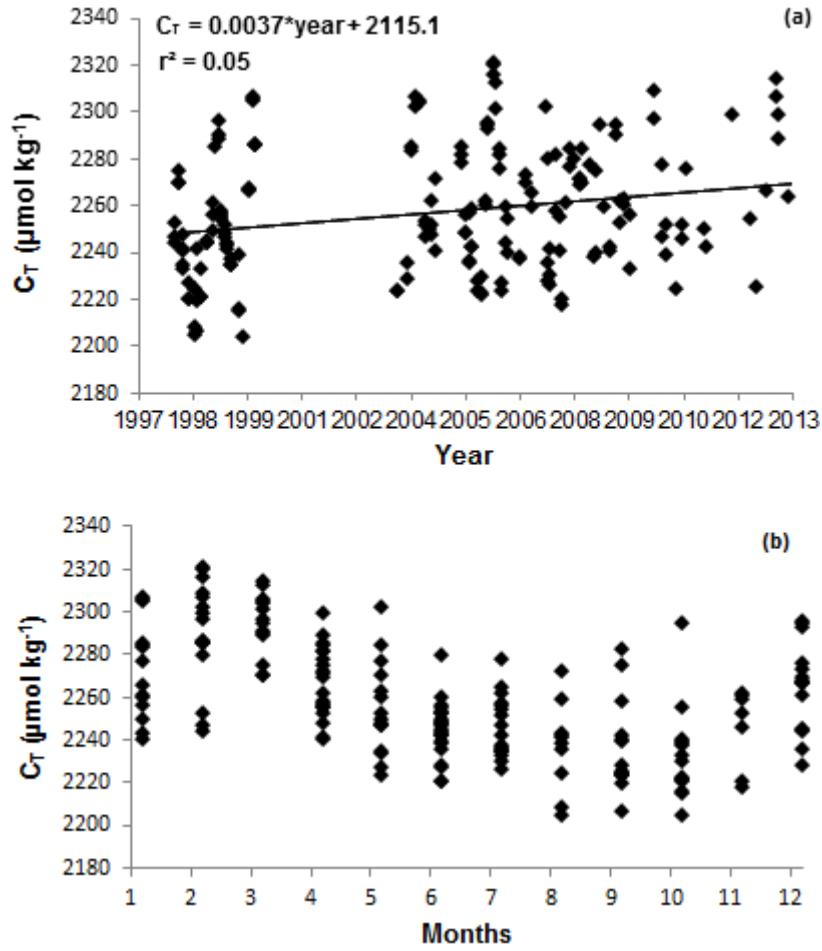
876
877 **Figure 2. Map of the residuals of the A_T algorithm (Eq 1) applied the (a) training and**
878 **(b) testing datasets**

879
880
881
882
883
884
885
886
887
888
889
890
891
892
893
894
895
896

897
898
899

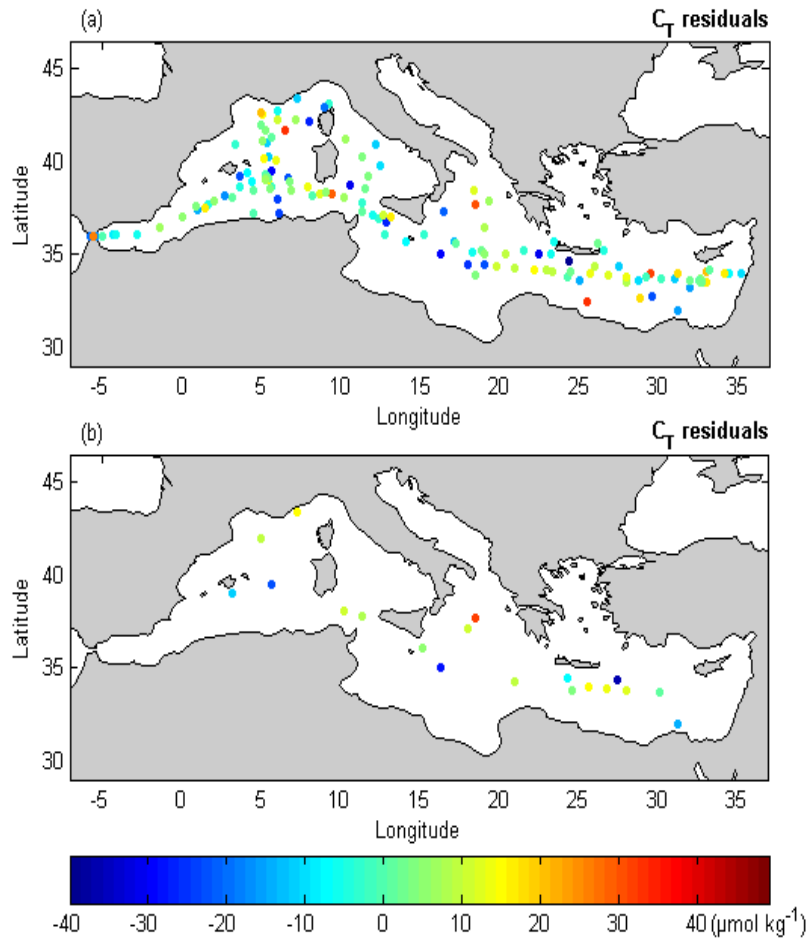


900
901 **Figure 3. Rate of increase applied to correct the C_T measurements in reference to the**
902 **year 2005**
903
904



905
 906
 907
 908
 909
 910
 911
 912
 913
 914
 915
 916
 917
 918
 919
 920
 921
 922
 923
 924
 925
 926

Figure 4. (a) Temporal and (b) seasonal variations of C_T measured at the Dyfamed time-series station between 1998 and 2013



927
 928
 929
 930
 931
 932
 933
 934
 935
 936
 937
 938
 939
 940
 941
 942
 943
 944
 945
 946

Figure 5. Comparison of the predicted C_T values from the C_T algorithm given in Eq (2) with measurements which are (a) included or (b) excluded when deriving the fit

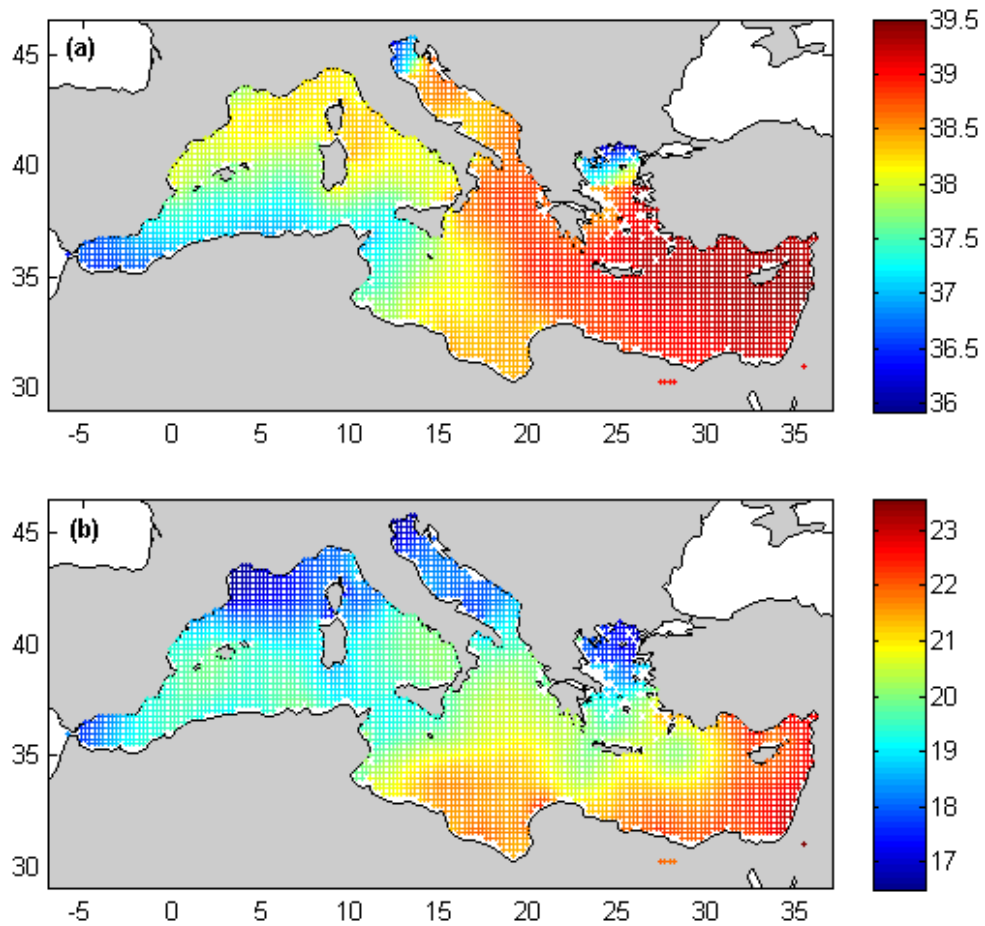


Figure 6. The seven years averages (2005-2012) of (a) SSS and (b) SST climatological fields of the WOA13 (Locarnini et al., 2013; Zweng et al., 2013)

947
 948
 949
 950
 951
 952
 953
 954
 955
 956
 957
 958
 959
 960
 961
 962
 963
 964
 965
 966
 967
 968

969
970
971
972
973
974
975
976
977
978
979
980
981
982
983
984
985
986
987
988
989
990
991
992
993
994
995
996
997
998
999
1000
1001
1002
1003
1004
1005
1006
1007
1008
1009
1010
1011
1012
1013
1014
1015

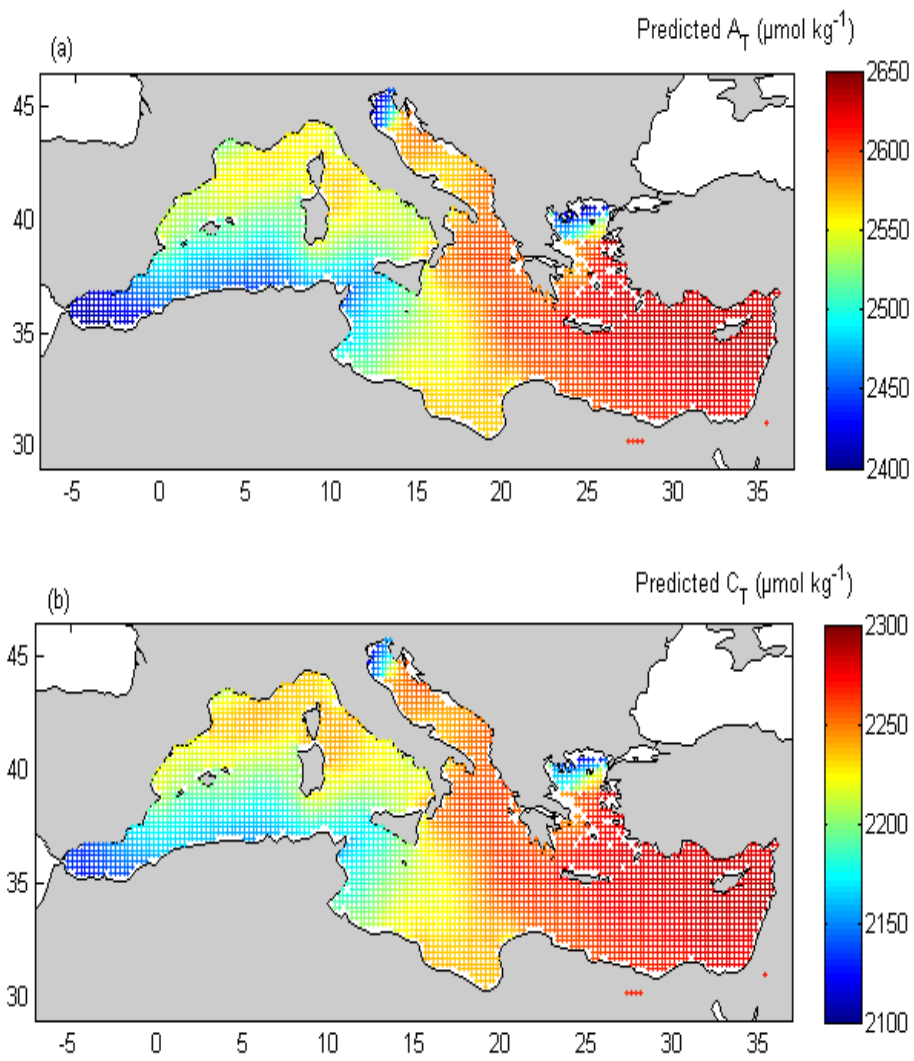
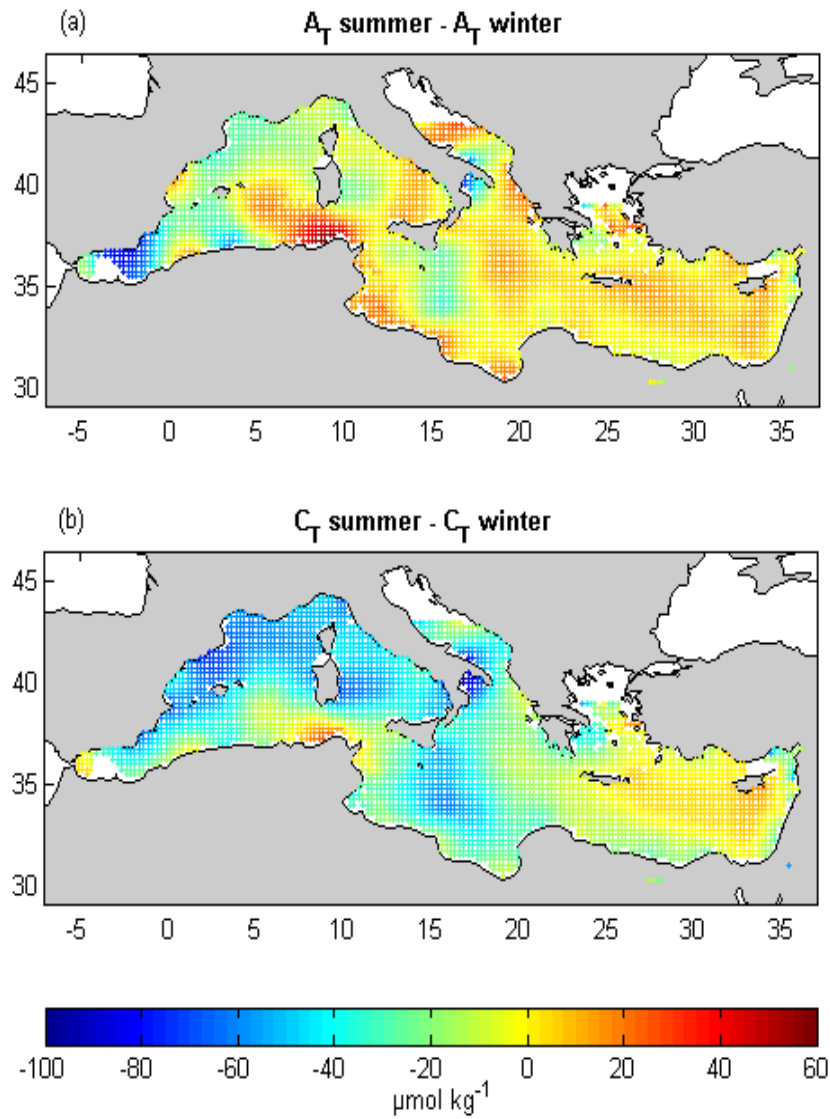


Figure 7. The seven years averages spatial variability of (a) surface A_T predicted from Eq (1) and (b) surface C_T predicted from Eq (2), applied to the 2005-2012 climatological fields of S and T from the WOA13



1016
 1017 **Figure 8. Distribution of the summer-winter differences of (a) surface A_T predicted**
 1018 **from Eq (1) and (b) surface C_T predicted from Eq (2), applied to the 2005-2012**
 1019 **climatological fields of S and T from the WOA13**

1020
 1021
 1022
 1023